When Age Tips the Balance: a Dual Mechanism Affecting Hemispheric Specialization for Language

Elise Roger[a,b,c,*,†], Loïc Labache[d,*,†], Noah Hamlin[e,f], Jordanna Kruse[e,f], Monica Baciu[c], Gaelle E. Doucet[e,f,g]

Aging engenders neuroadaptations, generally reducing specificity and selectivity in functional brain responses. Our investigation delves into the functional specialization of brain hemispheres within language-related networks across adulthood. In a cohort of 728 healthy adults spanning ages 18 to 88, we modeled the trajectories of inter-hemispheric asymmetry concerning the principal functional gradient across 37 homotopic regions of interest (hROIs) of an extensive language network, known as the Language-and-Memory Network. Our findings reveal that over two-thirds of Language-and-Memory Network hROIs undergo asymmetry changes with age, falling into two main clusters. The first cluster evolves from left-sided specialization to right-sided tendencies, while the second cluster transitions from right-sided asymmetry to left-hemisphere dominance. These reversed asymmetry shifts manifest around midlife, occurring after age 50, and are associated with poorer language production performance. Our results provide valuable insights into the influence of functional brain asymmetries on language proficiency and present a dynamic perspective on brain plasticity during the typical aging process.

Paul Pierre Broca challenged the prevailing 19th-century belief that the brain was organized holistically and symmetrically, providing evidence to support the idea that a prominently lateralized brain is a crucial characteristic for effectively carrying out certain cognitive functions, particularly language processing ("We speak with the left hemisphere," Broca, 1865, p. 384).

Patterns of hemispheric specialization and interaction of brain networks are complex, developmental, learning-dependent, and dynamic (Tzourio-Mazoyer & Seghier, 2016). From the earliest stages of development, human beings demonstrate behavioral and brain asymmetries – as early as ten weeks prenatal (Abu-Rustum et al., 2013) and 26 gestational weeks for perisylvian regions (Kasprian et al., 2011) – which become increasingly perceptible both functionally and anatomically during infancy. Asymmetries in neural networks take effect at different times during ontogeny, and almost all cortical brain regions show significant left-right asymmetries in adulthood (Kong et al., 2018). Language-related regions show covariate developmental trajectories (Leroy et al., 2011) and develop more slowly in the left hemisphere (LH) than in the right (Sowell et al., 2003). A notable right hemisphere (RH) language activation pattern in young children typically diminishes with age to become strongly left lateralized for most adults (Olulade et al., 2020). Examining the language connectome in adult populations and its organization across several language tasks reveals a pronounced left-hemispheric dominance in the central perisylvian network, which specializes in processing auditory-verbal stimuli (Roger, Rodrigues De Almeida, et al., 2022). This dominance of functional connectivity in the left hemisphere (LH) for the "core" language network has been consistently observed (Braga et al., 2020; Friederici, 2011; Labache et al., 2019; Vigneau et al., 2006).

However, language processing requires the involvement of a wider brain network, encompassing the core perisylvian LH system but also several peripheral or marginal memory, executive, and sensorimotor systems ((Hertrich et al., 2020), also discussed as multiple language networks by (Hagoort, 2017, 2019)). The extended language connectome comprises many fine-tuned associative hubs (Roger, Rodrigues De Almeida, et al., 2022). It is sharpened to underpin effective communication by integrating the high-level, multimodal perceptual and cognitive information required for language

[a] Institut Universitaire de Gériatrie de Montréal, Communication and Aging Lab, Montreal, Quebec, Canada. [b] Faculty of Medicine, University of Montreal, Montreal, Quebec, Canada. [c] Univ. Grenoble Alpes, Univ. Savoie Mont Blanc, CNRS, LPNC, 38000 Grenoble, France. [d] Department of Psychology, Yale University, New Haven, CT, 06520, US. [e] Institute for Human Neuroscience, Boys Town National Research Hospital, Omaha, NE, 68010, US. [f] Department of Pharmacology and Neuroscience, Creighton University School of Medicine, Omaha, NE, 68178, US. [g] Center for Pediatric Brain Health, Boys Town National Research Hospital, Omaha, NE, 68178, US. * Equal contribution (first author); these authors contributed equally to this study and can both list themselves as first author in their CVs. [†] Corresponding authors: Loïc Labache: loic.labache@yale.edu, Elise Roger: elise.roger@umontreal.ca.

processing (Roger, Banjac, et al., 2022). This sophisticated processing system is thus extremely powerful, yet it is also susceptible to vulnerabilities. Associative hubs are indeed highly prone to damage (Fornito et al., 2015), and ensuring the optimal function of language hubs in later life comes at a considerable cost (Baciu et al., 2016, 2021; Hoyau et al., 2018; Roger, Rodrigues De Almeida, et al., 2022). It is now well-documented that functional connectivity and network dynamics remodel with age (e.g., (G. E. Doucet et al., 2021; Goh, 2011; Sala-Llonch et al., 2015; Zonneveld et al., 2019). Importantly, older adults exhibit a default-executive coupling when engaged in demanding tasks, characterized by increased prefrontal involvement and reduced suppression of the Default Mode Network. In contrast, younger individuals adjust their functional responses by deactivating Default Mode Network regions when performing the same tasks (Buckner & DiNicola, 2019; Mazoyer et al., 2001; Shulman et al., 1997; Turner & Spreng, 2015). Overall, age-related changes are characterized by reduced specificity, selectivity, and lateralization of functional brain networks (Festini et al., 2018). Nevertheless, the trajectory of hemispheric specialization for language during aging, the underlying mechanisms involved, and their impact on cognition are still largely unclear and require further investigation.

Functional asymmetries can be investigated using intrinsic functional connectivity, which offers the advantage of abstracting from task-related variability associated with the nature and difficulty of specific tasks. Resting-state networks do exhibit spatial patterns that correspond with the networks observed during specific cognitive tasks (Cole et al., 2014, 2016; Ji et al., 2019)., and specific regions have been identified as already predisposed in language processing at rest (G. Doucet et al., 2011). Moreover, lateralization measures in key language hubs, derived from resting-state data, can predict functional lateralization during task performance (G. E. Doucet et al., 2015; Labache et al., 2020). Furthermore, recent studies on functional brain architecture have reported that resting-state networks exhibit a hierarchical organization characterized by smooth spatial transitions or gradients (Huntenburg et al., 2018; Margulies et al., 2016). The principal gradient (G1), explaining the most variance in whole-brain functional connectivity, aligns with established cortical hierarchies that progressively process complex or heteromodal information from sensory inputs ((Gonzalez Alam et al., 2022); see also (Chang et al., 2022) for natural language processing). Interestingly, the brain hemispheres do not show an identical pattern of organization on G1 (Liang et al., 2021), revealing a notable asymmetry for heteromodal networks linked to higher-order cognitive functions (Mancuso et al., 2019; Raemaekers et al., 2018). Furthermore, a recent study showed that individuals exhibiting atypical language lateralization display corresponding hemispheric differences in macroscale functional gradient organization, making G1 a marker of hemispheric specialization for language (Labache et al., 2023). Therefore, examining functional asymmetries within intricate networks, such as those supporting language processing, and how they change with age can bring a new perspective considering the fundamental underlying functional architecture.

Our study aimed to track how hemispheric asymmetry changes with age in the Language-and-Memory Network (Roger et al., 2020) using the functional principal gradient G1 based on resting-state data. To model the functional trajectories over an age range from 18 to 88 years, we applied the Generalized Additive Mixed Models (GAMMs) technique, which has been previously used in structural MRI studies (Roe et al., 2021a, 2023). This allowed us to classify Language-and-Memory Network regions based on their asymmetry patterns at rest throughout healthy aging. Furthermore, we also explored how these asymmetry changes were related to cognitive performance measured during various language tasks. To this end, we used Canonical Correlation Analyses (CCA) to assess how age impacted asymmetries in the language network across multimodal data, including anatomy, function, and cognitive performances.

Methods

Database demographics. The study sample comprised three datasets, accumulating 728 healthy adults (371 women) from 18 to 88 years old (μ=52.84 years, SD=19.19 years, Figure 1). Participants were included if they had a resting-state (rs) fMRI and structural MRI collected on a 3T MRI scanner.

The larger sample, the Cambridge Centre for Ageing and Neuroscience Project (Cam-CAN Project: www.mrc-cbu.cam.ac.uk, (Shafto et al., 2014)), included 627 participants (316 women). Further recruitment information and the acquisition parameters have been described elsewhere (Taylor et al., 2017). The sample mean age was 54.28 years (SD=18.61 years). Participants' handedness was defined based on the manual preference strength assessed with the Edinburgh inventory (Oldfield, 1971): participants with a score below 30 were considered left-handers (Hervé et al., 2006; Papadatou-Pastou et al., 2020), right-handers otherwise. The sample contained 56 left-handed participants (32 women). CamCAN funding was provided by the UK Biotechnology and Biological Sciences Research Council (grant number BB/H008217/1), with support from the UK Medical Research Council and the University of Cambridge, UK.

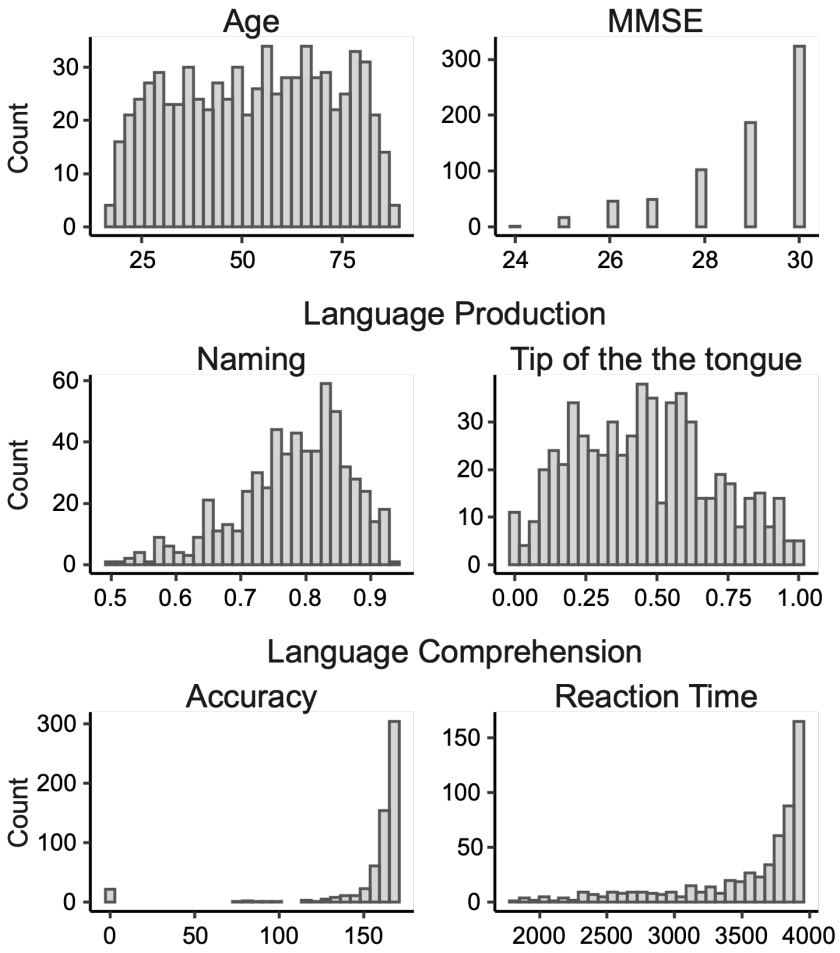

Figure 1 | Age and behavioral performance distributions (*n*=728). The behavioral tests assess various cognitive functions associated with language: word production, lexical access/retrieval abilities (picture Naming accuracy and Tip of the tongue ratio), and semantic and syntactic comprehension abilities (Accuracy and Reaction Time). A description of the behavioral variables is available as supplementary material in the article by West and colleagues (West et al., 2022). Reaction Time and Tip of the tongue performance were inverted, so all scores close to 0 represent worse performances.

The second sample was collected in Omaha, NE, USA, and included 54 participants (31 women). The acquisition parameters are fully described in (G. E. Doucet et al., 2022). Briefly, participants were scanned on a 3T Siemens Prisma scanner using a 64-channel head coil. Structural images were acquired using a T1-weighted, 3D magnetization-prepared rapid gradient-echo (MPRAGE) sequence with the following parameters: Repetition Time (TR)=2400 ms, Echo Time (TE)=2.22 ms, Field of View (FOV): 256×256 mm, matrix size: 320×320, 0.8 mm isotropic resolution, Inversion Time (TI)=1000 ms, 8 degree-flip angle, bandwidth=220 Hz/Pixel, echo spacing=7.5 ms, in-plane acceleration GRAPPA (GeneRalized Autocalibrating Partial Parallel Acquisition) factor 2, total acquisition time ~7 min. Participants also completed a resting-state fMRI scan using a multi-band T2* sequence with the following acquisition parameters: TR=800 ms, TE=37 ms, voxel size=2×2×2 mm^3, echo spacing 0.58 ms, bandwidth=2290 Hz/Pixel, number of axial slices = 72, multi-band acceleration factor=8, 460 volumes The sample mean age was 44.13 years (SD=19.07 years). Participants' handedness was self-reported: the sample contained seven left-handed participants (3 women). The study was approved by the Institutional Review Board for Research with Human Subjects at Boys Town National Research Hospital. Each participant provided written informed consent and completed the same protocol.

The third sample was collected in Grenoble, France, and included 47 participants (24 women). The acquisition parameters are described in (Roger et al., 2020). The sample mean age was 43.57 years (SD=21.92 years). Participants' handedness was self-reported: the sample contained two left-handed participants (1 woman). The ethics committee of the Grenoble Alpes University Hospital approved data collection (CPP 09-CHUG-14; MS-14-102).

We used the whole age range of the sample (*n*=728, 18-88 years) to model the asymmetry trajectories further throughout the lifespan.

Cognitive assessment of participants. For all 728 participants, we checked the Mini Mental State Examination (MMSE) scores to ensure that the general cognitive functioning of our sample remained within the expected range

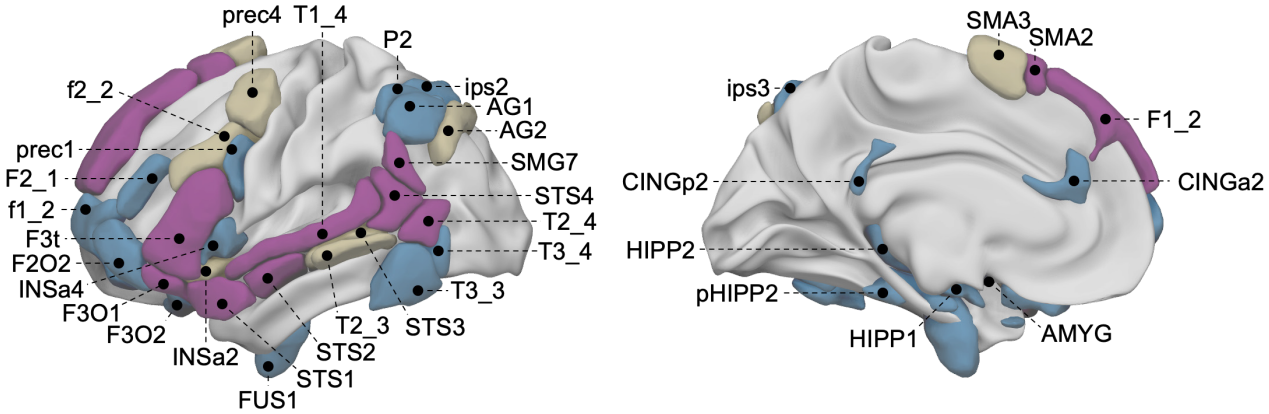

Figure 2 | Locations of the 37 regions of the Language-and-Memory Network atlas (Roger et al., 2020). *On the left:* Lateral view of the left hemisphere. *On the right:* Medial view of the left hemisphere. The atlas is composed of 74 homotopic ROIs (37 in each hemisphere) reported by two task-fMRI studies, one cross-sectional study for language (Labache et al., 2019), and one meta-analysis for memory (Spaniol et al., 2009) and adapted to the Atlas of Intrinsic Connectivity of Homotopic Areas coordinates (Joliot et al., 2015). Regions are rendered onto the 3D anatomical templates of the white matter surface of the left hemisphere in the MNI space with Surf Ice software (https://www.nitrc.org/projects/surfice/). Color code: purple, regions involved in language; blue, regions involved in episodic memory (encoding and retrieval); brown, regions involved in both language and memory. The Anterior Insula (3) (INSa3) is not visible on this render. See Table 1 for the correspondences between the abbreviations and the full names of the Language-and-Memory Network regions.

(Q_1=28, Q_3=30).

Among the three cohorts in our study, only the CamCAN cohort underwent an extensive set of behavioral assessments, resulting in cognitive data available for a specific sub-sample of 554 participants. These assessments, conducted outside the MRI scanner, are detailed in previous literature (Shafto et al., 2014, 2019; Samu et al., 2017; Taylor et al., 2017). We limited our analyses to language skill assessments only (Figure 1). We chose language-related measures because of their effectiveness in assessing diverse language-related aspects, encompassing word production, lexical access, and word retrieval (evaluated via picture naming accuracy and the tip-of-the-tongue ratio), as well as the understanding of semantics and syntax (measured through accuracy and reaction time). Further comprehensive descriptions of these behavioral variables are available in the supplementary materials provided by West and colleagues (West et al., 2022).

MRI Data Preprocessing. The neuroimaging data were formatted following the BIDS standard (Brain Imaging Data Structure - http://bids.neuroimaging.io/; (Gorgolewski et al., 2016; Roger et al., 2020)) and then preprocessed using the *fMRIPrep* software (https://fmriprep.org/en/stable/; (Esteban et al., 2019, 2020). The T1w preprocessing included skull stripping, tissue segmentation, and spatial normalization. Preprocessing of the rs-fMRI data followed the consensus steps for functional images, including motion correction, slice timing correction, susceptibility distortion correction, coregistration, and spatial normalization. The data were represented in the Montreal Neurological Institute (MNI) volumetric space. Finally, time series were extracted for each homotopic region of interest (hROIs; described in the following subsection) using Nilearn (https://nilearn.github.io/), with nuisance parameter regression. Confounding regression included cerebrospinal fluid and white matter signals and translation and rotation parameters for *x*, *y*, and *z* directions.

Language-and-Memory Network Statistics. Our statistical analyses were based on the Language-and-Memory Network atlas, an extended language network encompassing language-specific areas and related memory regions (Roger et al., 2020). Briefly, the Language-and-Memory Network comprises 37 homotopic regions of interest. Among these ten regions uniquely dedicated to the core supramodal language network (Labache et al., 2019), 19 supporting episodic memory (Spaniol et al., 2009), and eight regions underpinning both language and episodic memory processes. The core language network corresponded to a set of heteromodal brain regions significantly involved, leftward asymmetrical across three language contrasts (listening to, reading, and producing sentences), and functionally connected. The memory network was underpinned by areas that demonstrated strong activation patterns connected to episodic memory processes, such as encoding, effective recovery, and reminiscence. Figure 2 shows the Language-and-Memory Network in a brain rendering, and Table 1 lists all the Language-and-Memory Network regions. It should be noted that the language atlas was based on the AICHA atlas, a functional brain homotopic atlas optimized for studying functional brain asymmetries (Joliot et al.,

Abbreviation	Region	Function	MNI coordinates (left)			MNI coordinates (right)		
			X (*mm*)	Y (*mm*)	Z (*mm*)	X (*mm*)	Y (*mm*)	Z (*mm*)
AG1	Angular Gyrus (1)	M	-48	-57	44	51	-52	43
AG2	Angular Gyrus (2)	LM	-38	-70	39	45	-62	36
AMYG	Amygdala (1)	M	-22	0	-12	21	2	-12
CINGa2	Anterior Cingulate Gyrus (2)	M	-7	34	22	7	33	23
CINGp2	Posterior Cingulate Gyrus (2)	M	-4	-39	27	8	-43	31
f1_2	superior frontal sulcus (2)	M	-27	56	1	28	56	7
f2_2	inferior frontal sulcus (2)	LM	-43	15	29	44	19	28
F1_2	Superior Frontal Gyrus (2)	L	-12	46	41	12	45	42
F2_1	Middle Frontal Gyrus (1)	M	-40	41	20	41	44	13
F2O2	Middle Frontal Gyrus: Pars Orbitalis (2)	M	-41	49	-5	40	50	-4
F3O1	Inferior Frontal Gyrus: Pars Orbitalis (1)	L	-42	31	-17	44	33	-14
F3O2	Inferior Frontal Gyrus: Pars Orbitalis (2)	M	-21	23	-21	21	22	-20
F3t	Inferior Frontal Gyrus: Pars Triangularis (1)	L	-49	26	5	50	29	5
FUS1	Fusiform Gyrus (1)	M	-32	-9	-34	32	-8	-35
HIPP1	Hippocampal Gyrus (1)	M	-30	-7	-19	30	-5	-18
HIPP2	Hippocampal Gyrus (2)	M	-25	-32	-3	25	-31	-2
INSa2	Anterior Insula (2)	LM	-34	17	-13	35	18	-13
INSa3	Anterior Insula (3)	LM	-34	24	1	37	24	0
INSa4	Anterior Insula (4)	M	-41	15	3	41	15	4
ips2	intraparietal sulcus (2)	M	-34	-58	46	37	-52	48
ips3	intraparietal sulcus (3)	M	-27	-60	44	26	-62	46
P2	Inferior Parietal Gyrus (1)	M	-45	-53	50	43	-53	48
pHIPP2	Parahippocampal Gyrus (2)	M	-28	-27	-19	29	-25	-19
prec1	precentral sulcus (1)	M	-50	6	26	50	10	24
prec4	precentral sulcus (4)	LM	-42	1	50	44	1	48
SMA2	Supplementary Motor Area (2)	L	-11	18	63	11	18	63
SMA3	Supplementary Motor Area (3)	LM	-7	8	66	6	10	66
SMG7	Supramarginal Gyrus (7)	L	-55	-52	26	55	-46	33
STS1	superior temporal sulcus (1)	L	-50	14	-22	52	13	-26
STS2	superior temporal sulcus (2)	L	-55	-7	-13	54	-2	-15
STS3	superior temporal sulcus (3)	LM	-55	-33	-2	53	-32	0
STS4	superior temporal sulcus (4)	L	-57	-48	13	55	-46	15
T1_4	Superior Temporal Gyrus (4)	L	-59	-23	4	60	-20	2
T2_3	Middle Temporal Gyrus (3)	LM	-61	-35	-5	62	-31	-5
T2_4	Middle Temporal Gyrus (4)	L	-53	-59	7	57	-53	3
T3_3	Inferior Temporal Gyrus (3)	M	-56	-53	-14	57	-46	-14
T3_4	Inferior Temporal Gyrus (4)	M	-50	-61	-8	54	-58	-11

Table 1 | List of the Language-and-Memory network atlas regions. Note: L=language; LM=language and memory; M=memory; MNI coordinates, in the left and right hemisphere, of regions (*X*, *Y*, *Z*) in mm; Total regions=74 (37 in each hemisphere).

2015).

We computed two features characterizing the high-order Language-and-Memory Network hROIs (Roger et al., 2020) from the preprocessed neuroimaging data: the normalized volume and the first functional gradient (G1)

reflecting the macroscale functional organization of the cortex (Margulies et al., 2016). The first gradient captures the most variance of the correlations matrices (20%, 22%, and 19% for CamCAN, Omaha's, and Grenoble's cohorts, respectively). It has been previously shown to accurately reflect the lateralization of the language network (Labache et al., 2023).

Normalized Volume. Tissue segmentation was performed on the preprocessed T1w using the FreeSurfer pipeline (Version 6.0.0; CentOS Linux 6.10.i386). Briefly, the FreeSurfer segmentation process included the segmentation of the subcortical white matter and deep gray matter volumetric structures, intensity normalization, tessellation of the gray matter white matter boundary, automated topology correction, and surface deformation following intensity gradients to optimally place the gray/white and gray/cerebrospinal fluid borders at the location where the greatest shift in intensity defines the transition to the other tissue class. Structural volumes were normalized to total intracranial volume. Normalized volumes were extracted for each of the Language-and-Memory Network hROIs.

Connectivity Embedding. Each participant's values were obtained for the first functional gradient (G1). The gradients reflect participant connectivity matrices, reduced in their dimensionality through the approach of Margulies and colleagues (Margulies et al., 2016). Functional gradients reflect the topographical organization of the cortex in terms of sensory integration flow, as described by Mesulam (Mesulam, 1998). Gradients were computed using Python (Python version 3.8.10) and the BrainSpace library (Python package version 0.1.3 (Vos de Wael et al., 2020)). Gradients computed at the regional and vertex levels performed similarly (Vos de Wael et al., 2020).

Average region-level functional connectivity matrices were generated for each individual across the entire cortex (*i.e.*, 384 AICHA brain regions). Consistent with prior work, each region's top 10% connections were retained, and other elements in the matrix were set to 0 to enforce sparsity (Dong et al., 2021; Margulies et al., 2016). The normalized angle distance between any two rows of a matrix was calculated to obtain a symmetrical similarity matrix. Diffusion map embedding (Coifman et al., 2005; Coifman & Lafon, 2006; Lafon & Lee, 2006) was implemented on the similarity matrix to derive the first gradient. Note that the individual-level gradients were aligned using Procrustes rotation ($N_{iterations}$=10) to the corresponding group-level gradient. This alignment procedure was used to improve the similarity of the individual-level gradients to those from prior literature. Min-max normalization (0-100) was performed at the individual level for the whole brain (Gonzalez Alam et al., 2022).

Gradient asymmetry was then computed for each participant and region. For a given region, gradient asymmetry corresponded to the difference between the normalized gradient value in the left hemisphere minus the gradient values in the right hemisphere. A positive gradient asymmetry value meant a leftward asymmetry; a negative value meant a rightward asymmetry.

Statistical Analyses. Statistical analysis was performed using R (R version 4.2.2 (R Core Team, 2021)). Data wrangling was performed using the R library *dplyr* (R package version 1.0.10, (Wickham et al., 2023)). Graphs were realized using the R library *ggplot2* (R package version 3.4.2 (Wickham, 2016)). Brain visualizations were realized using Surf Ice (*NITRC: Surf Ice: Tool/resource Info, n.d.*).

Modeling Gradient Asymmetry Trajectories Throughout Life. For each region of the Language-and-Memory Network, we used factor-smooth Generalized Additive Mixed Models (GAMMs, as implemented in the R library *gamm4*; R package version 0.2-6 (Wood & Scheipl, 2020)) to fit a smooth gradient trajectory for Age per Hemisphere (Roe et al., 2021b, 2023) and to assess the smooth interaction between Hemisphere×Age within the clusters (see clusters definition below). Hemisphere was included as a fixed effect, while Sex and Site were treated as covariates of no interest. A random intercept for each subject was also included. GAMMs leverage smooth functions to model the non-linear trajectories of mean levels across individuals, providing robust estimates that can be applied to cross-sectional and longitudinal cognitive data (Sørensen et al., 2021). GAMMs were implemented using splines, a series of polynomial functions joined together at specific points, known as knots. The splines allow the smooth function to adapt its shape flexibly to the underlying pattern in the data across the range of the predictor variable. This connection allows for the modeling of complex, non-linear relationships piecewise while maintaining continuity and smoothness across the function. To minimize overfitting, the number of knots was constrained to be low (k=6). The significance of the smooth Hemisphere×Age interaction was assessed by testing for a difference in the smooth term of Age between hemispheres. We applied a False Discovery Rate correction (FDR, (Benjamini & Yekutieli, 2001)) to control for the number of tests conducted. Lastly, we used the linear predictor matrix of the GAMMs to obtain asymmetry trajectories underlying the interaction Hemisphere×Age and their confidence intervals. These were computed as the difference between zero-centered (*i.e.*, demeaned) hemispheric age trajectories.

Classification of Age-Asymmetry Trajectories. To classify the regions of the Language-

and-Memory Network found significant (after applying the FDR correction) according to their functional asymmetry skewness profile (*i.e.*, increasing leftward asymmetry from baseline, decreasing leftward asymmetry, or stabilizing asymmetry with age), we computed a dissimilarity matrix (sum of square differences) between all trajectories. We applied the Partition Around Medoids algorithm (PAM, R library *cluster*; R package version 2.1.4 (Maechler et al., 2022)) to identify clusters of regions sharing identical lifespan trajectories. Clustering solutions from two to seven were considered, and the mean silhouette width determined the optimal solution.

Canonical Correlation Analysis to Assess Brain–Behavior Associations. For each cluster, we assessed the linear relationship between the gradient asymmetry trajectories of the Language-and-Memory Network, their normalized volume, and cognitive language performance using permutation-based Canonical Correlation Analyses (CCA, (Wang et al., 2020)) inference. CCA is a multivariate statistical method identifying linear combinations of two sets of variables that correlate maximally. CCA reveals modes of joint variation, shedding light on the relationship between cognitive language performance (behavioral set), the lifespan trajectories of sensory integration flow asymmetry, and its underlying anatomy (brain set). The CCA results on a set of m mutually uncorrelated (*i.e.*, orthogonal) modes. Each mode captures a unique fraction of the multivariate brain and behavior covariation that isn't explained by any of the other $m-1$ modes. To assess statistical significance, we determined the robustness of each estimated CCA mode using permutation testing with 1,000 permutations. This test computes *p*-values to assess the null hypothesis of no correlation between components, adhering to the resampling method developed by Winker and colleagues (Winkler et al., 2020). *p*-values were controlled over Family-Wise Error Rate (FWER; FWER corrected *p*-values are denoted p_{FWER}), which is more appropriate than the FDR correction when measuring the significant canonical modes (Winkler et al., 2020).

Before conducting the CCA, we summarized the high-dimensional set of brain variables (gradient and normalized volume asymmetries) using principal component analysis (PCA, (Wang et al., 2020)). We retained components corresponding to the elbow point in the curve, representing the variance explained by each successive principal component. This was achieved using the R library *PCAtools* (R package version 2.5.15 (Blighe & Lun, 2021))). These retained principal components were then designated as the brain set for the CCA. Finally, we residualized the two variable sets (brain and behavior sets) to remove the influence of sex, age, and MMSE before executing the CCA.

The CCA had only been realized on the 554 participants of the CamCAN database due to a lack of behavioral data for other participants.

Results

Evolution of Hemispheric Gradient Asymmetries. To identify regions in the Language-and-Memory Network with changing gradient asymmetry across the lifespan, we applied GAMMs with Hemisphere×Age (*i.e.*, age-related change in asymmetry) as the effect of interest. This was done using combined data from 728 participants, aged 18 to 88, across cohorts.

Gradient significant age-related changes in asymmetry were found in 25 of the 37 regions of the Language-and-Memory Network (68% of the Language-and-Memory Network regions, all $p_{FDR}<0.024$, Figure 3). On the lateral surface of the temporal lobe, significant regions were localized alongside the superior temporal sulcus (STS1, STS2, STS3), extending to the Superior Temporal Gyrus dorsally (T1_4) and joining the posterior part of the Inferior Temporal Gyrus (T3_4) and ventrally, the Fusiform Gyrus (FUS4). Advancing toward the parietal lobe, the Supramarginal Gyrus (SMG7), the Inferior Parietal Gyrus (P2), and the intraparietal sulcus (ips3) also showed significant Hemisphere×Age interactions. On the lateral surface of the left frontal lobe, the regions showing a significant Hemisphere×Age interaction covered the *pars triangularis* part of the Inferior Frontal Gyrus (F3t), as well as the *pars orbitalis* (F2O2), the junction of the Middle Frontal Gyrus (F2_1) with the precentral sulcus (prec1, and prec4). The superior frontal sulcus (f1_2), the medial part of the Superior Frontal Gyrus (F1_2), and the pre-superior motor areas (SMA2 and SMA3) were also part of these areas in the frontal lobe. Three regions were located within the anterior Insula (INSa2, INSa3, and INSa4), while three others were located along the Hippocampal (HIPP1 and HIPP2) and paraHippocampal Gyri (pHIPP2). In the posterior medial wall, the Posterior Cingulum (CINGp2) was selected using this approach. The 12 non-significant regions (all $p_{FDR}>0.174$) were localized in the posterior part of the temporal (STS4, T2_3, T2_4, and T3_3) and the parietal lobes (AG1, AG2, and ips2), the anterior cingulate (CINGa2), the amygdala (AMYG), and the inferior frontal gyrus (F3_O1, F3_O2) and sulcus (f2_2).

Clustering of Asymmetry Trajectories. To investigate the asymmetry trajectories associated with the Hemisphere×Age interaction in the GAMMs, we conducted clustering on the 25 significant regions within the Language-and-Memory Network to pinpoint areas displaying similar patterns of gradient asymmetry changes throughout adulthood (Figure 3). The PAM algorithm identified two optimal partitions based on the mean silhouette width of 0.73. Including

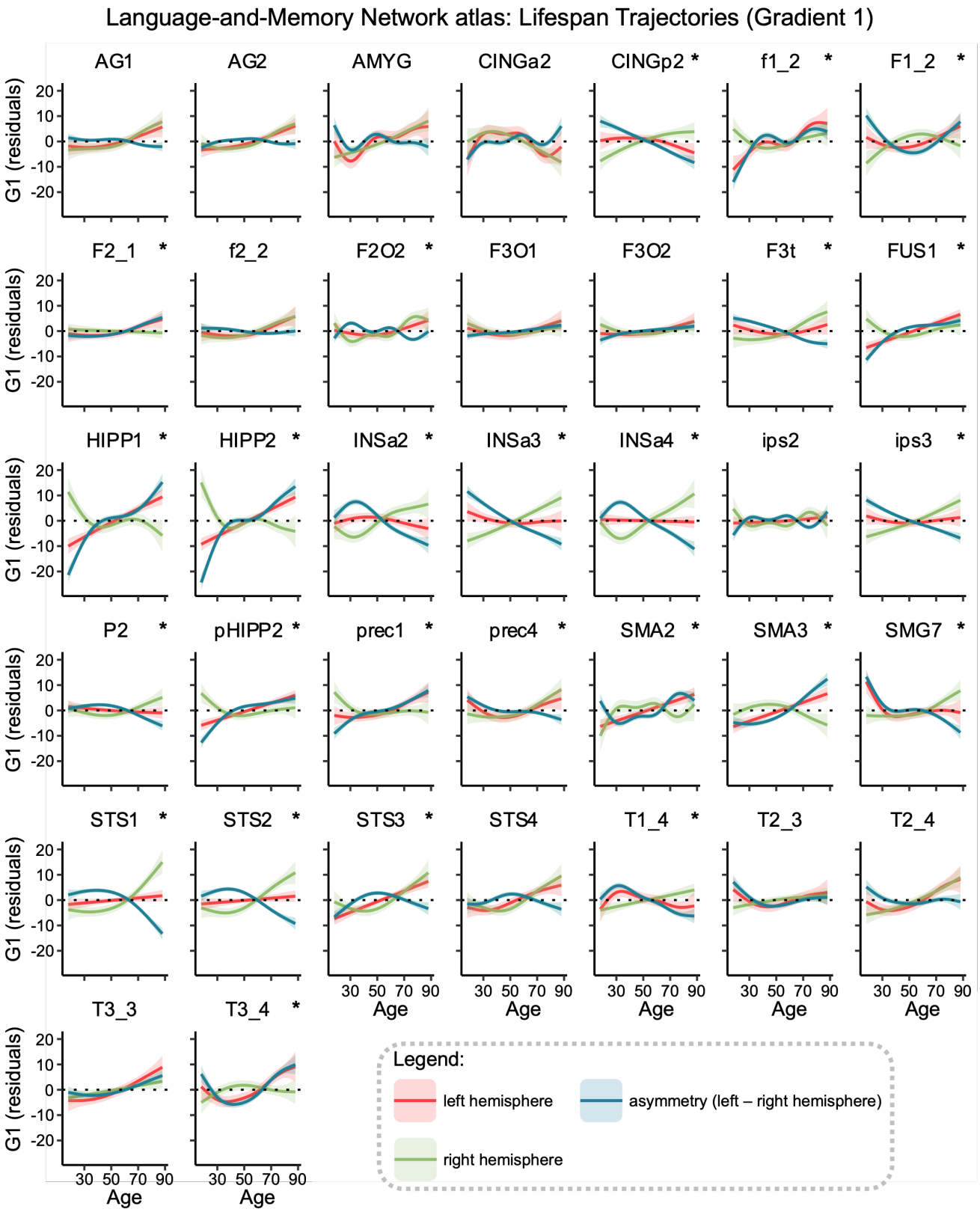

Figure 3 | Gradient lifespan trajectories of Language-and-Memory regions. Each region's graph shows the lifespan trajectory of the left (in red) and the right (in green) hemispheres and their asymmetry (in blue). Regions are plotted in alphabetical order. Trajectories were fitted using the generalized additive mixed models. Significant regions (pFDR<0.05) are marked with a star (*) in the top right corner. Data are residualized for sex, site, and random subject intercepts. Ribbons depict the standard error of the mean. The location of regions can be found in Figure 1. Correspondences between the abbreviations and the full names of a region can be found in Table 1.

the regions that did not exhibit significant changes in gradient asymmetries over the lifespan, the Language-and-Memory Network regions are grouped into three distinct clusters (Figure 4-A).

The first cluster, highlighted in light blue in Figure 4 and referenced similarly throughout the paper, comprised regions that showed an

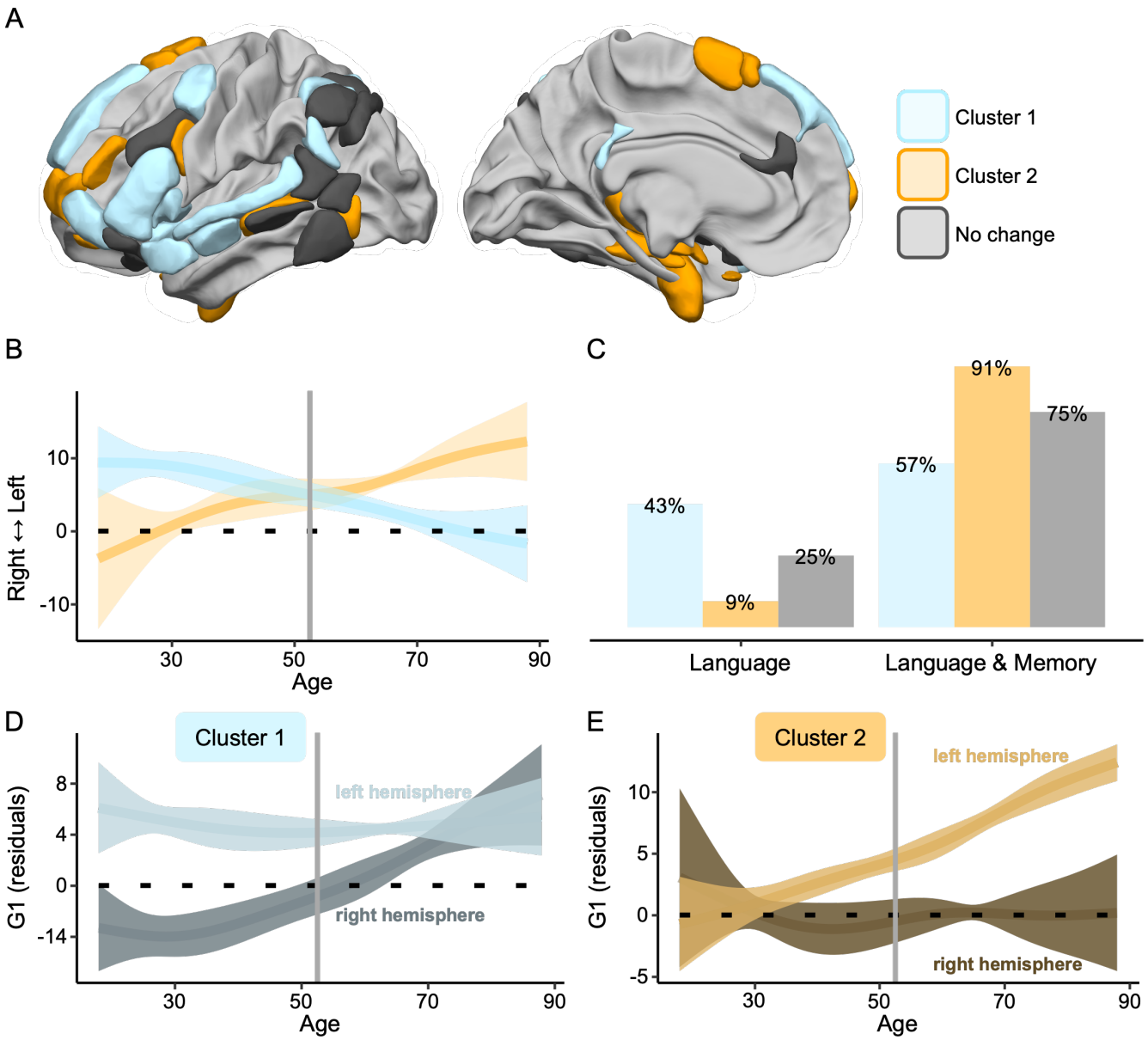

Figure 4 | Patterns of language-related neurocognitive trajectories. (A) The 25 Language-and-Memory Network regions associated with the two main clusters of change, categorized according to the *k*-medoids classification applied to the Euclidean distance matrix derived from the age-related curves of asymmetry as modeled by the Generalized Additive Mixed Model. Cluster 1, in blue, changes from left-sided dominant to bilateral. Cluster 2, in orange, changes from a bilateral organization to a left-side dominance. See Figure 2 and Table 1 for a description of the regions. **(B)** Average trajectory curves of the 1st gradient asymmetries from 18 to 88 years old. The two main patterns of inverse changes (Cluster 1 and Cluster 2) with age. The vertical line represents the intersection point between Cluster 1 and Cluster 2: 52.55 years old, *i.e.*, the age at which the 1st gradient asymmetry trends reverse. Ribbons depict the standard deviation. **(C)** The proportion of each cluster depends on the underlying cognitive processes: language or language and memory. **(D-E)** Modeling of the average estimated 1st gradient parameter for each hemisphere (left and right) across ages for Language-and-Memory Network regions belonging to Cluster 1 **(D)** and Cluster 2 **(E)**. Ribbons depict the standard deviation. The bilateralization of Cluster 1 with age is due to an increase of the 1st gradient values in the right hemisphere, while the left hemisphere remains stable. The left-sided specialization of Cluster 2 with age is due to an increase of the 1st gradient values in the left hemisphere, while the right hemisphere remains stable. This dual mechanism is mediated by an overspecialization of the contralateral hemisphere with age, characterized by an increased capacity to integrate high-level Language-and-Memory Network information.

average increase in their gradient values in the right hemisphere (Figure 4-D). These regions transitioned to a slightly rightward asymmetrical state with aging ($smooth_{88\ yo}$=-1.72), whereas they exhibited leftward asymmetry in earlier life stages ($smooth_{18\ yo}$=9.40, negative slope from positive intercept, Figure 4-B). The right hemisphere heteromodality increased significantly with aging, while the left hemisphere capacity remained stable. Within this cluster, 43% of the regions were dedicated to processing language, while 57% were multimodal, handling

language and memory functions (Figure 4-C). Cluster 1 regions are mapped onto the frontal, parietal, temporal, limbic cortices, and insula.

The second cluster, highlighted in light orange in Figure 4 and referenced similarly throughout the paper, comprised regions that showed an average increase in their gradient values in the left hemisphere (Figure 4-E). These regions transitioned to a leftward asymmetry state with aging ($smooth_{88\ yo}$=12.23), whereas they exhibited rightward asymmetry organization in earlier life stages ($smooth_{18\ yo}$=-3.77, positive slope from negative intercept, Figure 4-B). The left hemisphere heteromodal specialization increased significantly with aging, while the right hemisphere capacity remained stable. Within this cluster, 9% of the regions were dedicated to processing language, while 91% were multimodal, handling language and memory functions (Figure 4-C). Cluster 2 regions are mapped onto the frontal, temporal, and limbic cortices.

The last cluster (in grey in Figure 4), named "No change," regrouped the 12 non-significant regions that showed no significant changes in their hemispheric asymmetries throughout the lifespan. This cluster encompasses 25% of regions exclusively associated with language function and 75% of the regions involved in language and memory processes.

The trajectories of clusters 1 and 2 indicated that the asymmetry switch occurred at 52.6 years old (Figure 4-B). From this age onward, Cluster 2, which mainly encompasses multimodal regions, became the dominant leftward asymmetrical cluster. Its heteromodality in later life surpassed the early life heteromodality of Cluster 1. Meanwhile, Cluster 1 continued its decline towards a symmetrical organization of information integration.

Multimodal Brain-Cognition Association Change Analysis. We conducted a PCA on the brain set variables (gradient and normalized volume asymmetries) from the first cluster (Figure 4-A). This analysis indicated that the 28 variables could be condensed into four principal components, accounting for 49.79% of the total variance in the brain set. The first component alone explained 26.75% of the total variance and opposed the volume asymmetries of the dorsal language pathway regions to those of the ventral pathway regions (Figure 5-A, left column). Positive loadings then indicated a leftward asymmetry of the dorsal pathway, while negative ones indicated a rightward asymmetry of the ventral pathway. The second component alone explained 12.15% of the total variance. It opposed the volume asymmetries of the dorsal language pathway regions to those of the ventral pathway regions and the asymmetries of the first gradient (Figure 5-A, left column). Positive loadings then indicated a rightward asymmetry of the volume of the dorsal pathway regions and a leftward asymmetry of the ventral pathway as well as the gradient values. At the same time, negative loadings indicated the opposite pattern.

The multimodal canonical correlation analysis on the first cluster, which incorporated four brain metrics (principal components) and four behavioral metrics, revealed a single significant canonical correlation linking anatomy, function, and behavior ($p_{FWER}<1\times10^{-3}$). This brain mode accounted for 37.58% of the variance and primarily reflected the first and second components of the brain data set (Figure 5-B, left column). Positive values of the brain mode were associated with positive loading values for both the first and second principal components. Specifically, these positive values in the brain mode indicated a leftward asymmetry for all regions regarding gradient and normalized volume in the dorsal language pathway regions. Conversely, they represented a rightward asymmetry in the ventral pathway regions. The behavioral mode accounted for 39.47% of the variance and primarily reflected the naming and tip of the tongue tests (Figure 5-C, left column). Positive values of the behavioral mode were associated with better performances in language production. The correlation between the brain and behavioral modes was 0.28, as depicted in Figure 6 (left panel). Improved language production abilities were linked to a leftward asymmetry of the gradient value within the Language-and-Memory Network regions of the first cluster, a leftward asymmetry of the normalized volume for the dorsal language pathway regions, and a rightward asymmetry for the ventral language pathway regions.

The principal components analysis on the brain set variables (22 variables, gradient, and normalized volume asymmetries) for the second cluster (Figure 4-A) resulted in six principal components. Together, these principal components explained 59.35% of the total variance in the brain set. The first component alone explained 20.48% of the total variance and opposed the volume asymmetries of the mesial regions to those of the lateral side (Figure 5-A, right column). Positive loadings then indicated a rightward asymmetry of the normalized volume of the mesial regions and a leftward asymmetry of the lateral regions. Negative loadings indicated the opposite pattern. The second component alone explained 12.86% of the total variance and captured the asymmetry of the gradient, specifically, the asymmetry of the temporo-mesial memory-related regions (Figure 5-A, right column). Positive loadings indicated a rightward asymmetry of the gradient, while negative loadings indicated a leftward asymmetry.

The multimodal canonical correlation analysis on the second cluster, which incorporated six brain metrics (principal components) and four behavioral metrics, revealed a single

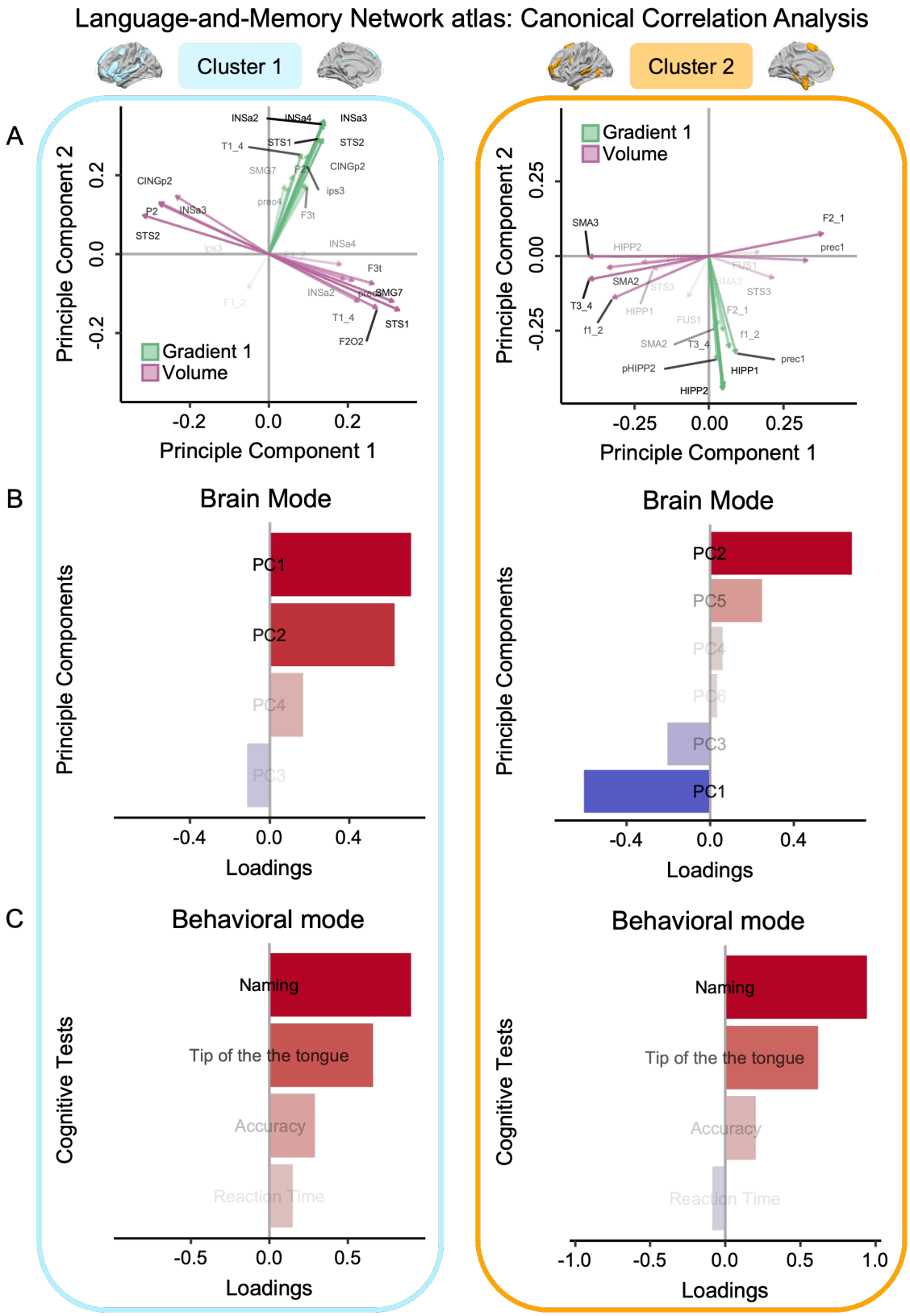

Figure 5 | Brain-behavior association using canonical correlation analysis. (A) Biplot of the principal component analysis of the regions belonging to Cluster 1 (*n*=14, on the left) and Cluster 2 (*n*=11, on the right). Each region was characterized by its asymmetry values of the 1st gradient and normalized volume. The two principal components of Cluster 1 explained 38.89% of the total variance (Principal Component 1=26.74%, Principal Component 2=12.15%). The two principal components of Cluster 2 explained 33.34% of the total variance (Principal Component 1=20.47%, Principal Component 2=12.87%). For Cluster 1, the 1st principal component opposed the volume asymmetries of the dorsal language pathway regions to the ventral semantic pathway regions. The 2sd component opposed the symmetries of the 1st gradient to the symmetries of the normalized volume. For Cluster 2, the 1st principal component opposed the asymmetry of mesial regions versus the volume asymmetry of lateral regions. The 2sd component coded for the symmetry of the 1st gradient, specifically, the symmetry of the temporo-mesial memory-related regions: a larger value meant a larger symmetry. **(B-C)** Overview of the canonical correlation analysis first modes. Only data from participants with all scores on the selected language indicators were included in the analysis (*n*=554;

← CamCAN cohort only). Sex, age, and general cognitive status (MMSE) were entered as covariates. **(B)** First mode for brain variables. For Cluster 1, the brain mode explained 38% of the variance. It is saturated by the first two components of the principal component analysis, mixing the multimodal biomarkers included in the analysis (1st gradient and normalized volume). For Cluster 2, the brain mode explained 24% of the variance. It is saturated by the first two components of the principal component analysis. **(C)** First mode of behavioral variables. For Cluster 1 and 2, the behavioral mode explained 39% of the variance and was saturated by the language production tasks involving lexical access and retrieval: naming and tip of the tongue. Results for Cluster 1 are framed in light blue. Results for Cluster 2 are framed in orange.

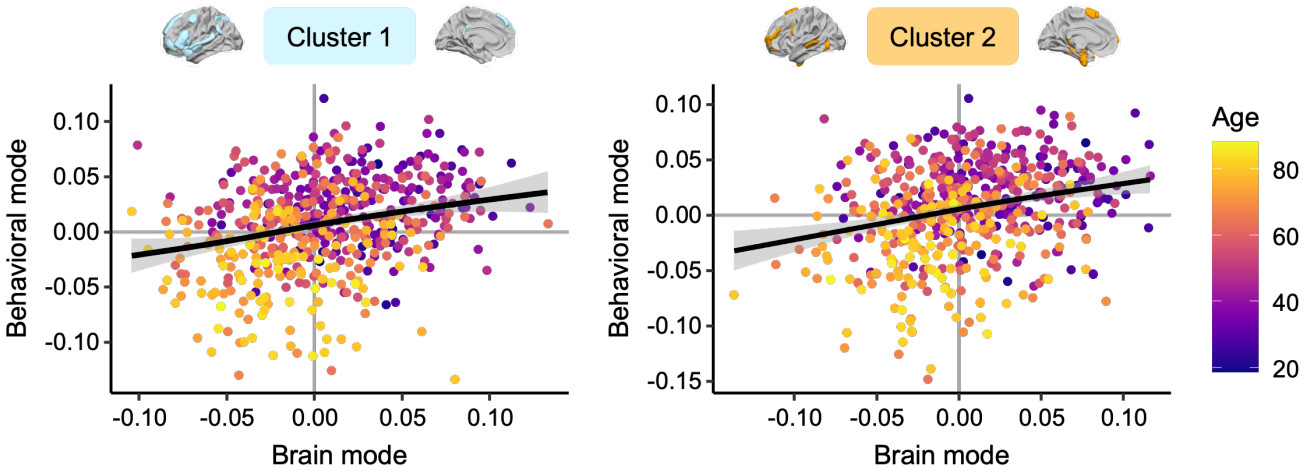

Figure 6 | Relationship between changes in inter-hemispheric balances and their behavioral implications in a multimodal perspective. The first brain and behavioral modes were significantly correlated for both clusters: r=0.28, p<1.10^{-3}. The significance of correlations between modes was assessed using permutation testing (n=1000). Color code for age.

significant canonical correlation linking anatomy, function, and behavior (p_{FWER}<1×10^{-3}). This brain mode accounted for 23.61% of the variance and opposed the second component of the brain data set to the first one (Figure 5-B, right column). Positive values of the brain mode were associated with positive loading values for the second component and negative values for the first component. A positive brain mode value meant a leftward asymmetry of the normalized volume of the mesial regions, a rightward asymmetry of the lateral regions, and a rightward asymmetry of the gradient. The behavioral mode accounted for 39.04% of the variance and, similarly to Cluster 1, primarily reflected the naming and tip of the tongue tests (Figure 5-C, right column). The correlation between the brain and behavioral modes was 0.28, as depicted in Figure 6 (right panel). Improved language production abilities were linked to a rightward asymmetry of the gradient value within the temporo-mesial memory-related regions, a leftward asymmetry of the normalized volume of the mesial regions, and a rightward asymmetry of the normalized volume of the lateral regions.

Discussion

The study's primary objective was to investigate the dynamics of functional asymmetry across the adult lifespan within an extended language network (Language-and-Memory Network). In young adults, our observations revealed a greater degree of heteromodality (G1) in the left hemisphere (LH) compared to the right hemisphere (RH) in the fronto-parietal regions forming the core language network. The limbic "memory" regions of the extended language network showed greater heteromodality in the RH (Figures 3 and 4B). These observations align with a recent investigation exploring brain-wide hemispheric preferences in the G1 principal gradient in young adults. Generally, associative networks exhibited higher levels of heteromodality in LH areas than their RH counterparts, except for the limbic temporal network, where the degree of heteromodality was higher in RH regions (Gonzalez Alam et al., 2022). These observations shed light on the differences in hemispheric asymmetry within specific networks.

To explore the dynamics of functional lateralization across the adult lifespan, we modeled the longitudinal trajectories of G1 hemispheric asymmetry changes from cross-sectional data with a method previously used to structural data in a comparable context (Roe et al., 2021b). It revealed that a substantial portion of the expanded language network experiences changes in how the brain hemispheres handle multimodal information as individuals age. Multiple distinct trajectories from the initial state have been observed (Figure 3), corresponding to two main patterns of change (Figure 4). Cluster 1 depicts regions that shift from an LH preference

in youth to a slight RH preference in old age. With healthy aging, homotopic regions of Cluster 1 become more heteromodal in the RH. The core language regions predominantly followed this trajectory (Figure 4C). On the other hand, Cluster 2 comprises regions that shift from an RH preference in youth to an LH preference with aging. As individuals age, there is an increase in the heteromodality of these regions within the LH. This trend was mainly observed in the Language-and-Memory Network regions that complement the core language network (Figure 4C).

We found that this dual mechanism of the Language-and-Memory Network neurofunctional imbalance in integrating complex, high-level information begins after age 50 and intensifies over time (Figure 4B). These findings are consistent with previous functional studies showing significant transitions in middle age (Hennessee et al., 2022). They also align with the onset of structural changes observed in healthy older adults regarding cortical thickness asymmetry, showing an accelerated loss of asymmetry after midlife (Fjell et al., 2010; Roe et al., 2021b; Vidal-Piñeiro et al., 2019). The reduction in structural asymmetry is notably significant in higher-order cortex and heteromodal regions, which may account for the extensive reorganization observed in the functional organization of the Language-and-Memory Network regions. None of these changes in asymmetry contributed to maintaining language performance with age and were, instead, linked to poorer performance. For Cluster 1 and Cluster 2, the pattern observed in young adults was related to more efficient language production (Figure 6), underlining the importance of specialization at all ages for effective interhemispheric cooperation. Consequently, the changes do not support the hypothesis of a compensatory phenomenon (see (Cabeza et al., 2018)), preserving language performance with age. On the contrary, it aligns with the dedifferentiation theory of aging (Li et al., 2009; Morcom & Friston, 2012; Morcom & Henson, 2018; Reuter-Lorenz & Lustig, 2005) and the brain maintenance theory (Nyberg, 2017; Nyberg et al., 2012), suggesting that maintaining a (functional) youthful brain state is an essential factor in cognitive preservation as individuals age. These findings further underscore Roe and colleagues' insights in their recent investigation of age-related shifts in functional asymmetry during memory retrieval (Roe et al., 2020).

The lateralization of individual functions, such as language, may be closely associated with the lateralization of many seemingly independent processes (Labache et al., 2023). Several studies suggest that the LH specialization for language may be linked to the concept of "complementary lateralization." This stands in contrast to the preferential specialization of the contralateral hemisphere (the RH) for other high-level cognitive functions like visuospatial processing (Badzakova-Trajkov et al., 2010; Cai et al., 2013; Cochet, 2016; Serrien & O'Regan, 2022; Zago et al., 2016). It has also been reported that the absence of functional lateralization for language production reduces performance in language tasks and other non-verbal, high-level functions (Mellet et al., 2014). The attentional and executive control networks (Yeo et al., 2011) play a role in maintaining these specializations, with LH control regions (Control-B) closer to the Default Mode Network (DMN-B) and RH attentional regions (DAN-B) nearer to the sensory-motor end of the gradient (Gonzalez Alam et al., 2022). Importantly, control networks undergo extensive reconfigurations during the aging process (e.g., see (Baciu et al., 2021; Betzel et al., 2014; G. E. Doucet et al., 2021; He et al., 2013; Mowinckel et al., 2012; Roger, Rodrigues De Almeida, et al., 2022)). These changes affect the substantial alterations observed in language's functional asymmetries and other cognitive functions. Although beyond the scope of this research, studying how changes in neurofunctional equiliburiums for different cognitive functions occur with age would offer invaluable insights into mutual network interactions.

The human brain typically exhibits marked structural left-right disparities, particularly pronounced in perisylvian regions associated with language. Although genetics contribute to these asymmetries, their impact appears to be less substantial than previously assumed, with heritability estimated at less than 30% in adults (Kong et al., 2018; Sha et al., 2021), suggesting that environmental factors likely play a substantial role. Current research points to two primary developmental trajectories: the first is primarily influenced by genetics and lays the groundwork for brain lateralization, while the second, built upon this genetic foundation, entails prolonged development in brain regions responsible for complex functions, rendering them more susceptible to the influence of environmental factors (Labache et al., 2023). The aging process, particularly affecting heteromodal associative brain regions in middle age, may introduce a phase of heightened vulnerability to environmental and life experience factors from this period onward. Pinpointing the specific environmental factors and midlife experiences that contribute to resilience or susceptibility in the face of changes in brain asymmetry holds the potential to enhance our understanding of the variability in neurocognitive aging. This may facilitate the development of personalized preventive measures and interventions for individuals at risk of experiencing accelerated aging. Importantly, functional asymmetry is not solely dependent on cognitive aspects but is also strongly influenced by sensory inputs (Hugdahl & Westerhausen, 2016; Van der Haegen et al., 2016). The decline of the peripheral nervous

system plays a pivotal role in triggering significant functional reconfigurations within the central nervous system (see (Huang et al., 2023); (Schulte et al., 2020) for the consequences of age-related hearing loss on the brain function). Furthermore, hearing impairment in midlife is a substantial risk factor for dementia, as emphasized in the 2020 report by the Lancet Commission on dementia prevention, intervention, and care (Livingston et al., 2020). By elucidating the intricate relationships between sensory inputs, neural adaptations, and cognitive aging, the investigation of bottom-up influences presents an intriguing yet relatively unexplored research avenue.

Several methodological considerations and potential biases require discussion. Our study isolated the effects of age from gender through statistical control. However, gender-based disparities in language-related functional connectivity have been reported (Roger, Rodrigues De Almeida, et al., 2022), alongside variations in the asymmetry of hemispheric functional gradients (Liang et al., 2021). Hence, future studies must delve into gender-specific characteristics of the extended language network. Furthermore, given that certain aspects of brain aging manifest disparities between males and females (e.g., (Goyal et al., 2019)), special consideration should be given to older adults since gender differences could be amplified. Moreover, our study predominantly included participants from WEIRD (Western, Educated, Industrialized, Rich, and Democratic) societies. Considering that most of the global population does not fit within this category (Henrich et al., 2010), it would be beneficial to replicate these findings in more diverse populations, considering the importance of cultural diversity in research. Resting-state functional MRI has gained popularity due to its strong association with task-based fMRI activations (Cole et al., 2014, 2016) and ease of acquisition, rendering it a valuable proxy for capturing functional neuronal processes. Nevertheless, the strength of hemispheric specialization for language depends on multiple factors, particularly the nature of the task (Bradshaw et al., 2017; Labache et al., 2019). Hence, conducting an additional study encompassing a diverse array of language-related functional tasks is essential to validate the consistency of the trends observed in our resting-state functional data. Open fMRI databases dedicated to language, such as InLang (Roger, Rodrigues De Almeida, et al., 2022), could facilitate such investigations. However, the databases available to date only sometimes include a wide age range, which could limit insights into older adults. Finally, longitudinal data are imperative for providing conclusive evidence regarding evolutionary trajectories throughout the lifespan and their cognitive implications. The STAC-r model (revised Scaffolding Theory of Aging and Cognition model) emphasizes the importance of examining cognitive changes within individuals (Reuter-Lorenz & Park, 2014). This approach helps distinguish between mechanisms that maintain brain integrity and compensatory processes. Both mechanisms are crucial for preserving cognition in older adults, as noted by Reuter-Lorenz and Park in 2014. However, the current scarcity of extensive longitudinal cohorts, spanning both older and younger adults, hinders the identification of features predictive of future brain function and cognitive preservation (G. E. Doucet et al., 2022). It would also be important to extend the study to cohorts with mild cognitive impairment (MCI) and related conditions, which is crucial for assessing the specificity of the observed effects and discerning trends across different conditions.

Conclusion

Functional asymmetry in integrating high-level information optimization plays a crucial role in the functioning of neural processes involved in language. Examining these patterns over time revealed shifts in hemispheric predominances, emphasizing the dynamic nature of functional lateralization. Changes in asymmetries are linked to the language production challenges frequently observed in typical aging, challenging the idea of a compensatory function for the heightened engagement of the opposite hemisphere in aging. Instead, our findings align with the brain maintenance theory, highlighting the importance of sustaining a youthful functional brain state for optimal cognitive performance as individuals age. This study expands upon previous research on interhemispheric reorganization and opens avenues for a deeper understanding of the dynamic processes through which the brain and cognition adapt during aging.

Code Availability

The atlas and the code used to produce the results and visualizations can be found here (Labache, Roger, et al., 2023): https://github.com/loiclabache/RogerLabache_2023_LanguAging.

Disclosure Statement

The authors declare no actual or potential conflict of interest.

CRediT Authorship Contribution Statement

Elise Roger: Conceptualization, Data curation, Formal analysis, Investigation, Methodology, Software, Validation, Visualization, Writing - original draft, Writing - review & editing. **Loïc Labache:** Conceptualization, Data curation,

Formal analysis, Methodology, Software, Validation, Visualization, Writing - original draft, Writing - review & editing. **Noah Hamlin:** Data curation, Investigation. **Jordanna Kruse:** Data curation, Investigation. **Monica Baciu:** Conceptualization, Data curation, Funding acquisition, Investigation, Methodology, Resources, Supervision, Writing - review & editing. **Gaelle E. Doucet:** Conceptualization, Data curation, Funding acquisition, Investigation, Supervision, Writing - review & editing.

Funding

E.R. received funding support from the Canadian Institutes of Health Research (CIHR), the "Fonds de Recherche du Québec - Santé" (FRQS), and the AGE-WELL Canadian network. This work was supported by the grant NeuroCoG IDEX UGA in the framework of the "Investissements d'avenir" program (ANR-15-IDEX-02 to M.B.), by the French program "AAP GENERIQUE 2017" run by the "Agence Nationale pour la Recherche" (ANR-17-CE28–0015-01 to M.B.) and by the Institut Universitaire de France (M.B.), as well as by the following awards to G.E.D.: the National Institutes of Health (P20GM144641, R03AG064001). The content is solely the responsibility of the authors and does not necessarily represent the official views of the National Institutes of Health.

References

Abu-Rustum, R. S., Ziade, M. F., & Abu-Rustum, S. E. (2013). Reference values for the right and left fetal choroid plexus at 11 to 13 weeks: an early sign of "developmental" laterality? Journal of Ultrasound in Medicine: Official Journal of the American Institute of Ultrasound in Medicine, 32(9), 1623–1629.

Baciu, M., Banjac, S., Roger, E., Haldin, C., Perrone-Bertolotti, M., Lœvenbruck, H., & Démonet, J.-F. (2021). Strategies and cognitive reserve to preserve lexical production in aging. GeroScience, 43(4), 1725–1765.

Baciu, M., Boudiaf, N., Cousin, E., Perrone-Bertolotti, M., Pichat, C., Fournet, N., Chainay, H., Lamalle, L., & Krainik, A. (2016). Functional MRI evidence for the decline of word retrieval and generation during normal aging. Age , 38(1), 3.

Badzakova-Trajkov, G., Häberling, I. S., Roberts, R. P., & Corballis, M. C. (2010). Cerebral asymmetries: complementary and independent processes. PloS One, 5(3), e9682.

Benjamini, Y., & Yekutieli, D. (2001). The control of the false discovery rate in multiple testing under dependency. Annals of Statistics, 29(4), 1165–1188.

Betzel, R. F., Byrge, L., He, Y., Goñi, J., Zuo, X.-N., & Sporns, O. (2014). Changes in structural and functional connectivity among resting-state networks across the human lifespan. NeuroImage, 102 Pt 2, 345–357.

Blighe, K., & Lun, A. (2021). PCAtools: PCAtools: Everything Principal Components Analysis. https://github.com/kevinblighe/PCAtools

Bradshaw, A. R., Thompson, P. A., Wilson, A. C., Bishop, D. V. M., & Woodhead, Z. V. J. (2017). Measuring language lateralisation with different language tasks: a systematic review. PeerJ, 5, e3929.

Braga, R. M., DiNicola, L. M., Becker, H. C., & Buckner, R. L. (2020). Situating the left-lateralized language network in the broader organization of multiple specialized large-scale distributed networks. Journal of Neurophysiology, 124(5), 1415–1448.

Buckner, R. L., & DiNicola, L. M. (2019). The brain's default network: updated anatomy, physiology and evolving insights. Nature Reviews. Neuroscience, 20(10), 593–608.

Cabeza, R., Albert, M., Belleville, S., Craik, F. I. M., Duarte, A., Grady, C. L., Lindenberger, U., Nyberg, L., Park, D. C., Reuter-Lorenz, P. A., Rugg, M. D., Steffener, J., & Rajah, M. N. (2018). Maintenance, reserve and compensation: the cognitive neuroscience of healthy ageing. Nature Reviews. Neuroscience, 19(11), 701–710.

Cai, Q., Van der Haegen, L., & Brysbaert, M. (2013). Complementary hemispheric specialization for language production and visuospatial attention. Proceedings of the National Academy of Sciences of the United States of America, 110(4), E322–E330.

Chang, C. H. C., Nastase, S. A., & Hasson, U. (2022). Information flow across the cortical timescale hierarchy during narrative construction. Proceedings of the National Academy of Sciences of the United States of America, 119(51), e2209307119.

Cochet, H. (2016). Manual asymmetries and hemispheric specialization: Insight from developmental studies. Neuropsychologia, 93(Pt B), 335–341.

Coifman, R. R., & Lafon, S. (2006). Diffusion maps. Applied and Computational Harmonic Analysis, 21(1), 5–30.

Coifman, R. R., Lafon, S., Lee, A. B., Maggioni, M., Nadler, B., Warner, F., & Zucker, S. W. (2005). Geometric diffusions as a tool for harmonic analysis and structure definition of data: diffusion maps. Proceedings of the National Academy of Sciences of the United States of America, 102(21), 7426–7431.

Cole, M. W., Bassett, D. S., Power, J. D., Braver, T. S., & Petersen, S. E. (2014). Intrinsic and task-evoked network architectures of the human brain. Neuron, 83(1), 238–251.

Cole, M. W., Ito, T., Bassett, D. S., & Schultz, D. H. (2016). Activity flow over resting-state networks shapes cognitive task activations. Nature Neuroscience, 19(12), 1718–1726.

Dong, H.-M., Margulies, D. S., Zuo, X.-N., &

Holmes, A. J. (2021). Shifting gradients of macroscale cortical organization mark the transition from childhood to adolescence. Proceedings of the National Academy of Sciences of the United States of America, 118(28). https://doi.org/10.1073/pnas.2024448118

Doucet, G. E., Hamlin, N., West, A., Kruse, J. A., Moser, D. A., & Wilson, T. W. (2022). Multivariate patterns of brain-behavior associations across the adult lifespan. Aging, 14(1), 161–194.

Doucet, G. E., Labache, L., Thompson, P. M., Joliot, M., Frangou, S., & Alzheimer's Disease Neuroimaging Initiative. (2021). Atlas55+: Brain Functional Atlas of Resting-State Networks for Late Adulthood. Cerebral Cortex , 31(3), 1719–1731.

Doucet, G. E., Pustina, D., Skidmore, C., Sharan, A., Sperling, M. R., & Tracy, J. I. (2015). Resting-state functional connectivity predicts the strength of hemispheric lateralization for language processing in temporal lobe epilepsy and normals. Human Brain Mapping, 36(1), 288–303.

Doucet, G., Naveau, M., Petit, L., Delcroix, N., Zago, L., Crivello, F., Jobard, G., Tzourio-Mazoyer, N., Mazoyer, B., Mellet, E., & Joliot, M. (2011). Brain activity at rest: a multiscale hierarchical functional organization. Journal of Neurophysiology, 105(6), 2753–2763.

Esteban, O., Ciric, R., Finc, K., Blair, R. W., Markiewicz, C. J., Moodie, C. A., Kent, J. D., Goncalves, M., DuPre, E., Gomez, D. E. P., Ye, Z., Salo, T., Valabregue, R., Amlien, I. K., Liem, F., Jacoby, N., Stojić, H., Cieslak, M., Urchs, S., … Gorgolewski, K. J. (2020). Analysis of task-based functional MRI data preprocessed with fMRIPrep. Nature Protocols, 15(7), 2186–2202.

Esteban, O., Markiewicz, C. J., Blair, R. W., Moodie, C. A., Isik, A. I., Erramuzpe, A., Kent, J. D., Goncalves, M., DuPre, E., Snyder, M., Oya, H., Ghosh, S. S., Wright, J., Durnez, J., Poldrack, R. A., & Gorgolewski, K. J. (2019). fMRIPrep: a robust preprocessing pipeline for functional MRI. Nature Methods, 16(1), 111–116.

Festini, S. B., Zahodne, L., & Reuter-Lorenz, P. A. (2018). Theoretical perspectives on age differences in brain activation: HAROLD, PASA, CRUNCH—how do they STAC up? In Oxford Research Encyclopedia of Psychology. Oxford University Press. https://doi.org/10.1093/acrefore/9780190236557.013.400

Fjell, A. M., Walhovd, K. B., Westlye, L. T., Østby, Y., Tamnes, C. K., Jernigan, T. L., Gamst, A., & Dale, A. M. (2010). When does brain aging accelerate? Dangers of quadratic fits in cross-sectional studies. NeuroImage, 50(4), 1376–1383.

Friederici, A. D. (2011). The brain basis of language processing: from structure to function. Physiological Reviews, 91(4), 1357–1392.

Goh, J. O. S. (2011). Functional Dedifferentiation and Altered Connectivity in Older Adults: Neural Accounts of Cognitive Aging. Aging and Disease, 2(1), 30–48.

Gonzalez Alam, T. R. D. J., Mckeown, B. L. A., Gao, Z., Bernhardt, B., Vos de Wael, R., Margulies, D. S., Smallwood, J., & Jefferies, E. (2022). A tale of two gradients: differences between the left and right hemispheres predict semantic cognition. Brain Structure & Function, 227(2), 631–654.

Gorgolewski, K. J., Auer, T., Calhoun, V. D., Craddock, R. C., Das, S., Duff, E. P., Flandin, G., Ghosh, S. S., Glatard, T., Halchenko, Y. O., Handwerker, D. A., Hanke, M., Keator, D., Li, X., Michael, Z., Maumet, C., Nichols, B. N., Nichols, T. E., Pellman, J., … Poldrack, R. A. (2016). The brain imaging data structure, a format for organizing and describing outputs of neuroimaging experiments. Scientific Data, 3, 160044.

Goyal, M. S., Blazey, T. M., Su, Y., Couture, L. E., Durbin, T. J., Bateman, R. J., Benzinger, T. L.-S., Morris, J. C., Raichle, M. E., & Vlassenko, A. G. (2019). Persistent metabolic youth in the aging female brain. Proceedings of the National Academy of Sciences of the United States of America, 116(8), 3251–3255.

Hagoort, P. (2017). The core and beyond in the language-ready brain. Neuroscience and Biobehavioral Reviews, 81(Pt B), 194–204.

Hagoort, P. (2019). The neurobiology of language beyond single-word processing. Science, 366(6461), 55–58.

Hennessee, J. P., Webb, C. E., Chen, X., Kennedy, K. M., Wig, G. S., & Park, D. C. (2022). Relationship of prefrontal brain lateralization to optimal cognitive function differs with age. NeuroImage, 264, 119736.

Henrich, J., Heine, S. J., & Norenzayan, A. (2010). Most people are not WEIRD. Nature, 466(7302), 29.

Hertrich, I., Dietrich, S., & Ackermann, H. (2020). The margins of the language network in the brain. Frontiers in Communication, 5. https://doi.org/10.3389/fcomm.2020.519955

Hervé, P.-Y., Crivello, F., Perchey, G., Mazoyer, B., & Tzourio-Mazoyer, N. (2006). Handedness and cerebral anatomical asymmetries in young adult males. NeuroImage, 29(4), 1066–1079.

He, X., Qin, W., Liu, Y., Zhang, X., Duan, Y., Song, J., Li, K., Jiang, T., & Yu, C. (2013). Age-related decrease in functional connectivity of the right fronto-insular cortex with the central executive and default-mode networks in adults from young to middle age. Neuroscience Letters, 544, 74–79.

Hoyau, E., Roux-Sibilon, A., Boudiaf, N., Pichat,

C., Cousin, E., Krainik, A., Jaillard, A., Peyrin, C., & Baciu, M. (2018). Aging modulates fronto-temporal cortical interactions during lexical production. A dynamic causal modeling study. Brain and Language, 184, 11–19.

Huang, H.-M., Chen, G.-S., Liu, Z.-Y., Meng, Q.-L., Li, J.-H., Dong, H.-W., Chen, Y.-C., Zhao, F., Tang, X.-W., Gao, J.-L., Chen, X.-M., Cai, Y.-X., & Zheng, Y.-Q. (2023). Age-related hearing loss accelerates the decline in fast speech comprehension and the decompensation of cortical network connections. Neural Regeneration Research, 18(9), 1968–1975.

Hugdahl, K., & Westerhausen, R. (2016). Speech processing asymmetry revealed by dichotic listening and functional brain imaging. Neuropsychologia, 93(Pt B), 466–481.

Huntenburg, J. M., Bazin, P.-L., & Margulies, D.S. (2018). Large-Scale Gradients in Human Cortical Organization. Trends in Cognitive Sciences, 22(1), 21–31.

Ji, J. L., Spronk, M., Kulkarni, K., Repovš, G., Anticevic, A., & Cole, M. W. (2019). Mapping the human brain's cortical-subcortical functional network organization. NeuroImage, 185, 35–57.

Joliot, M., Jobard, G., Naveau, M., Delcroix, N., Petit, L., Zago, L., Crivello, F., Mellet, E., Mazoyer, B., & Tzourio-Mazoyer, N. (2015). AICHA: An atlas of intrinsic connectivity of homotopic areas. Journal of Neuroscience Methods, 254, 46–59.

Kasprian, G., Langs, G., Brugger, P. C., Bittner, M., Weber, M., Arantes, M., & Prayer, D. (2011). The prenatal origin of hemispheric asymmetry: an in utero neuroimaging study. Cerebral Cortex , 21(5), 1076–1083.

Kong, X.-Z., Mathias, S. R., Guadalupe, T., ENIGMA Laterality Working Group, Glahn, D. C., Franke, B., Crivello, F., Tzourio-Mazoyer, N., Fisher, S. E., Thompson, P. M., & Francks, C. (2018). Mapping cortical brain asymmetry in 17,141 healthy individuals worldwide via the ENIGMA Consortium. Proceedings of the National Academy of Sciences of the United States of America, 115(22), E5154–E5163.

Labache, L., Ge, T., Yeo, B. T. T., & Holmes, A. J. (2023). Language network lateralization is reflected throughout the macroscale functional organization of cortex. Nature Communications, 14(1), 3405.

Labache, L., Joliot, M., Saracco, J., Jobard, G., Hesling, I., Zago, L., Mellet, E., Petit, L., Crivello, F., Mazoyer, B., & Tzourio-Mazoyer, N. (2019). A SENtence Supramodal Areas AtlaS (SENSAAS) based on multiple task-induced activation mapping and graph analysis of intrinsic connectivity in 144 healthy right-handers. Brain Structure & Function, 224(2), 859–882.

Labache, L., Mazoyer, B., Joliot, M., Crivello, F., Hesling, I., & Tzourio-Mazoyer, N. (2020). Typical and atypical language brain organization based on intrinsic connectivity and multitask functional asymmetries. eLife, 9. https://doi.org/10.7554/eLife.58722

Labache, L., Roger, E., Hamlin, N., Kruse, J., Baciu, M., & Doucet, G. E. (2023). When Age Tips the Balance: a Dual Mechanism Affecting Hemispheric Specialization for Language. RogerLabache_2023_LanguAging. Zenodo. https://doi.org/10.5281/ZENODO.10253278

Lafon, S., & Lee, A. B. (2006). Diffusion maps and coarse-graining: A unified framework for dimensionality reduction, graph partitioning, and data set parameterization. IEEE Transactions on Pattern Analysis and Machine Intelligence, 28(9), 1393–1403.

Leroy, F., Glasel, H., Dubois, J., Hertz-Pannier, L., Thirion, B., Mangin, J.-F., & Dehaene-Lambertz, G. (2011). Early maturation of the linguistic dorsal pathway in human infants. The Journal of Neuroscience: The Official Journal of the Society for Neuroscience, 31(4), 1500–1506.

Liang, X., Zhao, C., Jin, X., Jiang, Y., Yang, L., Chen, Y., & Gong, G. (2021). Sex-related human brain asymmetry in hemispheric functional gradients. NeuroImage, 229, 117761.

Livingston, G., Huntley, J., Sommerlad, A., Ames, D., Ballard, C., Banerjee, S., Brayne, C., Burns, A., Cohen-Mansfield, J., Cooper, C., Costafreda, S. G., Dias, A., Fox, N., Gitlin, L. N., Howard, R., Kales, H. C., Kivimäki, M., Larson, E. B., Ogunniyi, A., ... Mukadam, N. (2020). Dementia prevention, intervention, and care: 2020 report of the Lancet Commission. The Lancet, 396(10248), 413–446.

Li, Z., Moore, A. B., Tyner, C., & Hu, X. (2009). Asymmetric connectivity reduction and its relationship to "HAROLD" in aging brain. Brain Research, 1295, 149–158.

Maechler, M., Rousseeuw, P., Struyf, A., Hubert, M., & Hornik, K. (2022). cluster: Cluster Analysis Basics and Extensions. https://CRAN.R-project.org/package=cluster

Mancuso, L., Costa, T., Nani, A., Manuello, J., Liloia, D., Gelmini, G., Panero, M., Duca, S., & Cauda, F. (2019). The homotopic connectivity of the functional brain: a meta-analytic approach. Scientific Reports, 9(1), 3346.

Margulies, D. S., Ghosh, S. S., Goulas, A., Falkiewicz, M., Huntenburg, J. M., Langs, G., Bezgin, G., Eickhoff, S. B., Castellanos, F. X., Petrides, M., Jefferies, E., & Smallwood, J. (2016). Situating the default-mode network along a principal gradient of macroscale cortical organization. Proceedings of the National Academy of Sciences of the United States of America, 113(44), 12574–12579.

Mazoyer, B., Zago, L., Mellet, E., Bricogne, S., Etard, O., Houdé, O., Crivello, F., Joliot, M.,

Petit, L., & Tzourio-Mazoyer, N. (2001). Cortical networks for working memory and executive functions sustain the conscious resting state in man. Brain Research Bulletin, 54(3), 287–298.

Mellet, E., Zago, L., Jobard, G., Crivello, F., Petit, L., Joliot, M., Mazoyer, B., & Tzourio-Mazoyer, N. (2014). Weak language lateralization affects both verbal and spatial skills: an fMRI study in 297 subjects. Neuropsychologia, 65, 56–62.

Mesulam, M. M. (1998). From sensation to cognition. Brain: A Journal of Neurology, 121 (Pt 6), 1013–1052.

Morcom, A. M., & Friston, K. J. (2012). Decoding episodic memory in ageing: a Bayesian analysis of activity patterns predicting memory. NeuroImage, 59(2), 1772–1782.

Morcom, A. M., & Henson, R. N. A. (2018). Increased Prefrontal Activity with Aging Reflects Nonspecific Neural Responses Rather than Compensation. The Journal of Neuroscience: The Official Journal of the Society for Neuroscience, 38(33), 7303–7313.

Mowinckel, A. M., Espeseth, T., & Westlye, L. T. (2012). Network-specific effects of age and in-scanner subject motion: a resting-state fMRI study of 238 healthy adults. NeuroImage, 63(3), 1364–1373.

NITRC: Surf ice: Tool/resource info. (n.d.). Retrieved March 24, 2022, from http://www.nitrc.org/projects/surfice/

Nyberg, L. (2017). Neuroimaging in aging: brain maintenance. F1000Research, 6, 1215.

Nyberg, L., Lövdén, M., Riklund, K., Lindenberger, U., & Bäckman, L. (2012). Memory aging and brain maintenance. Trends in Cognitive Sciences, 16(5), 292–305.

Oldfield, R. C. (1971). The assessment and analysis of handedness: the Edinburgh inventory. Neuropsychologia, 9(1), 97–113.

Olulade, O. A., Seydell-Greenwald, A., Chambers, C. E., Turkeltaub, P. E., Dromerick, A. W., Berl, M. M., Gaillard, W. D., & Newport, E. L. (2020). The neural basis of language development: Changes in lateralization over age. Proceedings of the National Academy of Sciences of the United States of America, 117(38), 23477–23483.

Papadatou-Pastou, M., Ntolka, E., Schmitz, J., Martin, M., Munafò, M. R., Ocklenburg, S., & Paracchini, S. (2020). Human handedness: A meta-analysis. Psychological Bulletin, 146(6), 481–524.

Raemaekers, M., Schellekens, W., Petridou, N., & Ramsey, N. F. (2018). Knowing left from right: asymmetric functional connectivity during resting state. Brain Structure & Function, 223(4), 1909–1922.

R Core Team. (2021). R: A language and environment for statistical computing. R Foundation for Statistical Computing. https://www.R-project.org/

Reuter-Lorenz, P. A., & Lustig, C. (2005). Brain aging: reorganizing discoveries about the aging mind. Current Opinion in Neurobiology, 15(2), 245–251.

Reuter-Lorenz, P. A., & Park, D. C. (2014). How does it STAC up? Revisiting the scaffolding theory of aging and cognition. Neuropsychology Review, 24(3), 355–370.

Roe, J. M., Vidal-Pineiro, D., Amlien, I. K., Pan, M., Sneve, M. H., Thiebaut de Schotten, M., Friedrich, P., Sha, Z., Francks, C., Eilertsen, E. M., Wang, Y., Walhovd, K. B., Fjell, A. M., & Westerhausen, R. (2023). Tracing the development and lifespan change of population-level structural asymmetry in the cerebral cortex. eLife, 12. https://doi.org/10.7554/eLife.84685

Roe, J. M., Vidal-Piñeiro, D., Sneve, M. H., Kompus, K., Greve, D. N., Walhovd, K. B., Fjell, A. M., & Westerhausen, R. (2020). Age-Related Differences in Functional Asymmetry During Memory Retrieval Revisited: No Evidence for Contralateral Overactivation or Compensation. Cerebral Cortex , 30(3), 1129–1147.

Roe, J. M., Vidal-Piñeiro, D., Sørensen, Ø., Brandmaier, A. M., Düzel, S., Gonzalez, H. A., Kievit, R. A., Knights, E., Kühn, S., Lindenberger, U., Mowinckel, A. M., Nyberg, L., Park, D. C., Pudas, S., Rundle, M. M., Walhovd, K. B., Fjell, A. M., Westerhausen, R., & Australian Imaging Biomarkers and Lifestyle Flagship Study of Ageing. (2021a). Asymmetric thinning of the cerebral cortex across the adult lifespan is accelerated in Alzheimer's disease. Nature Communications, 12(1), 721.

Roe, J. M., Vidal-Piñeiro, D., Sørensen, Ø., Brandmaier, A. M., Düzel, S., Gonzalez, H. A., Kievit, R. A., Knights, E., Kühn, S., Lindenberger, U., Mowinckel, A. M., Nyberg, L., Park, D. C., Pudas, S., Rundle, M. M., Walhovd, K. B., Fjell, A. M., Westerhausen, R., & Australian Imaging Biomarkers and Lifestyle Flagship Study of Ageing. (2021b). Asymmetric thinning of the cerebral cortex across the adult lifespan is accelerated in Alzheimer's disease. Nature Communications, 12(1), 721.

Roger, E., Banjac, S., Thiebaut de Schotten, M., & Baciu, M. (2022). Missing links: The functional unification of language and memory (LUM). Neuroscience and Biobehavioral Reviews, 133, 104489.

Roger, E., Pichat, C., Torlay, L., David, O., Renard, F., Banjac, S., Attyé, A., Minotti, L., Lamalle, L., Kahane, P., & Baciu, M. (2020). Hubs disruption in mesial temporal lobe epilepsy. A resting-state fMRI study on a language-and-memory network. Human Brain Mapping, 41(3), 779–796.

Roger, E., Rodrigues De Almeida, L., Loevenbruck, H., Perrone-Bertolotti, M., Cousin, E., Schwartz, J. L., Perrier, P., Dohen, M., Vilain, A., Baraduc, P., Achard, S., & Baciu,

M. (2022). Unraveling the functional attributes of the language connectome: crucial subnetworks, flexibility and variability. NeuroImage, 263, 119672.

Sala-Llonch, R., Bartrés-Faz, D., & Junqué, C. (2015). Reorganization of brain networks in aging: a review of functional connectivity studies. Frontiers in Psychology, 6, 663.

Schulte, A., Thiel, C. M., Gieseler, A., Tahden, M., Colonius, H., & Rosemann, S. (2020). Reduced resting state functional connectivity with increasing age-related hearing loss and McGurk susceptibility. Scientific Reports, 10(1), 16987.

Serrien, D. J., & O'Regan, L. (2022). The interactive functional biases of manual, language and attention systems. Cognitive Research: Principles and Implications, 7(1), 20.

Shafto, M. A., Tyler, L. K., Dixon, M., Taylor, J.R., Rowe, J. B., Cusack, R., Calder, A. J., Marslen-Wilson, W. D., Duncan, J., Dalgleish, T., Henson, R. N., Brayne, C., Matthews, F. E., & Cam-CAN. (2014). The Cambridge Centre for Ageing and Neuroscience (Cam-CAN) study protocol: a cross-sectional, lifespan, multidisciplinary examination of healthy cognitive ageing. BMC Neurology, 14, 204.

Sha, Z., Pepe, A., Schijven, D., Carrión-Castillo, A., Roe, J. M., Westerhausen, R., Joliot, M., Fisher, S. E., Crivello, F., & Francks, C. (2021). Handedness and its genetic influences are associated with structural asymmetries of the cerebral cortex in 31,864 individuals. Proceedings of the National Academy of Sciences of the United States of America, 118(47). https://doi.org/10.1073/pnas.2113095118

Shulman, G. L., Fiez, J. A., Corbetta, M., Buckner, R. L., Miezin, F. M., Raichle, M. E., & Petersen, S. E. (1997). Common Blood Flow Changes across Visual Tasks: II. Decreases in Cerebral Cortex. Journal of Cognitive Neuroscience, 9(5), 648–663.

Sørensen, Ø., Walhovd, K. B., & Fjell, A. M. (2021). A recipe for accurate estimation of lifespan brain trajectories, distinguishing longitudinal and cohort effects. NeuroImage, 226, 117596.

Sowell, E. R., Peterson, B. S., Thompson, P. M., Welcome, S. E., Henkenius, A. L., & Toga, A. W. (2003). Mapping cortical change across the human life span. Nature Neuroscience, 6(3), 309–315.

Spaniol, J., Davidson, P. S. R., Kim, A. S. N., Han, H., Moscovitch, M., & Grady, C. L. (2009). Event-related fMRI studies of episodic encoding and retrieval: meta-analyses using activation likelihood estimation. Neuropsychologia, 47(8-9), 1765–1779.

Taylor, J. R., Williams, N., Cusack, R., Auer, T., Shafto, M. A., Dixon, M., Tyler, L. K., Cam-Can, & Henson, R. N. (2017). The Cambridge Centre for Ageing and Neuroscience (Cam-CAN) data repository: Structural and functional MRI, MEG, and cognitive data from a cross-sectional adult lifespan sample. NeuroImage, 144(Pt B), 262–269.

Turner, G. R., & Spreng, R. N. (2015). Prefrontal Engagement and Reduced Default Network Suppression Co-occur and Are Dynamically Coupled in Older Adults: The Default-Executive Coupling Hypothesis of Aging. Journal of Cognitive Neuroscience, 27(12), 2462–2476.

Tzourio-Mazoyer, N., & Seghier, M. L. (2016). The neural bases of hemispheric specialization. Neuropsychologia, 93(Pt B), 319–324.

Van der Haegen, L., Acke, F., Vingerhoets, G., Dhooge, I., De Leenheer, E., Cai, Q., & Brysbaert, M. (2016). Laterality and unilateral deafness: Patients with congenital right ear deafness do not develop atypical language dominance. Neuropsychologia, 93(Pt B), 482–492.

Vidal-Piñeiro, D., Sneve, M. H., Nyberg, L. H., Mowinckel, A. M., Sederevicius, D., Walhovd, K. B., & Fjell, A. M. (2019). Maintained Frontal Activity Underlies High Memory Function Over 8 Years in Aging. Cerebral Cortex , 29(7), 3111–3123.

Vigneau, M., Beaucousin, V., Hervé, P. Y., Duffau, H., Crivello, F., Houdé, O., Mazoyer, B., & Tzourio-Mazoyer, N. (2006). Meta-analyzing left hemisphere language areas: phonology, semantics, and sentence processing. NeuroImage, 30(4), 1414–1432.

Vos de Wael, R., Benkarim, O., Paquola, C., Lariviere, S., Royer, J., Tavakol, S., Xu, T., Hong, S.-J., Langs, G., Valk, S., Misic, B., Milham, M., Margulies, D., Smallwood, J., & Bernhardt, B. C. (2020). BrainSpace: a toolbox for the analysis of macroscale gradients in neuroimaging and connectomics datasets. Communications Biology, 3(1), 103.

Wang, H.-T., Smallwood, J., Mourao-Miranda, J., Xia, C. H., Satterthwaite, T. D., Bassett, D. S., & Bzdok, D. (2020). Finding the needle in a high-dimensional haystack: Canonical correlation analysis for neuroscientists. NeuroImage, 216, 116745.

West, A., Hamlin, N., Frangou, S., Wilson, T. W., & Doucet, G. E. (2022). Person-Based Similarity Index for Cognition and Its Neural Correlates in Late Adulthood: Implications for Cognitive Reserve. Cerebral Cortex , 32(2), 397–407.

Wickham, H. (2016). ggplot2: Elegant Graphics for Data Analysis. Springer.

Wickham, H., François, R., Henr, y. L., Müller, K., & Vaughan, D. (2023). dplyr: A Grammar of Data Manipulation (Version 1.0.10). https://dplyr.tidyverse.org; https://github.com/tidyverse/dplyr

Winkler, A. M., Renaud, O., Smith, S. M., & Nichols, T. E. (2020). Permutation inference for canonical correlation analysis. NeuroImage, 220, 117065.

Wood, S., & Scheipl, F. (2020). gamm4:

Generalized additive mixed models using mgcv and lme4 (Version 0.2-6). https://CRAN.R-project.org/package=gamm4

Yeo, B. T. T., Krienen, F. M., Sepulcre, J., Sabuncu, M. R., Lashkari, D., Hollinshead, M., Roffman, J. L., Smoller, J. W., Zöllei, L., Polimeni, J. R., Fischl, B., Liu, H., & Buckner, R. L. (2011). The organization of the human cerebral cortex estimated by intrinsic functional connectivity. Journal of Neurophysiology, 106(3), 1125–1165.

Zago, L., Petit, L., Mellet, E., Jobard, G., Crivello, F., Joliot, M., Mazoyer, B., & Tzourio-Mazoyer, N. (2016). The association between hemispheric specialization for language production and for spatial attention depends on left-hand preference strength. Neuropsychologia, 93(Pt B), 394–406.

Zonneveld, H. I., Pruim, R. H., Bos, D., Vrooman, H. A., Muetzel, R. L., Hofman, A., Rombouts, S. A., van der Lugt, A., Niessen, W. J., Ikram, M. A., & Vernooij, M. W. (2019). Patterns of functional connectivity in an aging population: The Rotterdam Study. NeuroImage, 189, 432–444.